Am J Transl Res 2026;18(9):8314-8327
www.ajtr.org /ISSN:1943-8141/AJTR0174474

Original Article

Diosgenin suppresses colorectal cancer cell malignancy by modulating the AKT1/IL-6/STAT3 signaling axis

Yumo Yuan[1], Jiayi Li[2], Yina Lu[3]

[1]*School of Elderly Care Services and Management, Nanjing University of Chinese Medicine, Nanjing 210023, Jiangsu, China;* [2]*School of Medicine, Nanjing University of Chinese Medicine, Nanjing 210023, Jiangsu, China;* [3]*School of Integrative Medicine, Nanjing University of Chinese Medicine, Nanjing 210023, Jiangsu, China*

Received June 3, 2026; Accepted August 28, 2026; Epub September 15, 2026; Published September 30, 2026

Abstract: Objective: To investigate whether diosgenin inhibits the proliferation, migration, and invasion of colorectal cancer cells and to elucidate the underlying molecular mechanisms. Methods: CCK-8 assays were used to evaluate the viability of HCT116 and SW480 cells and determine the half-maximal inhibitory concentration (IC_{50}) values. Transwell assays were performed to assess cell migration and invasion. Apoptosis and protein expression levels were evaluated using flow cytometry and Western blotting (WB). The expression of AKT1/IL-6/STAT3 signaling pathway-related molecules was analyzed using WB, ELISA, and qRT-PCR. Functional rescue experiments were performed using the AKT1 inhibitor MK-2206, AKT1-specific siRNA, exogenous IL-6, and the STAT3 blocker Stattic. Nuclear translocation of phosphorylated AKT1 (P-AKT1) and P-STAT3 was examined by immunofluorescence. Results: Diosgenin decreased the viability of HCT116 and SW480 cells in a dose-dependent manner, suppressed cell migration and invasion, induced apoptosis, and modulated the Bax/Bcl-2 and Caspase-3/PARP apoptotic pathways. Mechanistically, diosgenin suppressed AKT1 phosphorylation, thereby reducing IL-6 excretion and inhibiting STAT3 activation. AKT1 inhibitor or siRNA knockdown both enhanced the inhibitory effects of diosgenin on cell viability, whereas exogenous IL-6 partially reversed these effects. In addition, the STAT3 inhibitor exhibited a synergistic effect with diosgenin. Immunofluorescence analysis demonstrated that diosgenin reduced the nuclear translocation of P-AKT1 and P-STAT3. Conclusion: Diosgenin suppresses the proliferation, migration and invasion of colorectal cancer cells and induces mitochondrial-mediated apoptosis by inhibiting the AKT1/IL-6/STAT3 signaling pathway. These findings provide experimental evidence supporting the use of diosgenin in the treatment of colorectal cancer.

Keywords: Diosgenin, colorectal cancer, AKT1/IL-6/STAT3 signaling axis, apoptosis, migration, invasion

Introduction

Colorectal cancer (CRC) remains a major global health burden [1-3]. According to 2024 Global Cancer Observatory (GLOBOCAN) data, approximately 1.926 million new cases and 0.904 million deaths attributable to CRC occur annually worldwide, and it has the highest lifetime risk among gastrointestinal cancers, reaching approximately 38.5% [3]. Despite the implementation of screening programs and advances in surgical treatment, the 5-year survival rate for metastatic colorectal cancer (mCRC) remains limited, ranging from 10-25% [4, 5]. Therefore, increasing efforts have been devoted to elucidating the molecular mechanisms underlying CRC progression and developing novel therapeutic strategies.

AKT1, a key component of the PI3K/AKT signaling pathway, is often overexpressed in CRC and promotes tumor growth and metastasis by regulating cell proliferation and metabolism [6-8]. Previous studies have demonstrated that aberrant activation of the AKT1 pathway is closely linked to CRC initiation, progression, and poor outcomes [9, 10]. Additionally, IL-6, a representative inflammatory cytokine, is significantly elevated in both the serum and tumor microenvironment of CRC patients, where it promotes cancer cell proliferation, migration, and invasion through activation of the downstream STAT3 signaling pathway [11, 12]. Persistent activation of the IL-6/STAT3 axis has been reported to facilitate CRC progression [9, 13]. AKT1 and the IL-6/STAT3 signaling network are also closely interconnected; AKT1 can increase

https://doi.org/10.62347/JGOP3511

IL-6 production and secretion through multiple mechanisms, thereby activating STAT3 and establishing a positive feedback loop [14-16]. Therefore, targeting the AKT1/IL-6/STAT3 signaling pathways has recently attracted increasing attention as a potential therapeutic strategy for colorectal cancer.

Chinese herbal medicine, with diverse pharmacologically active components and relatively low toxicity, have been extensively investigated in cancer treatment in recent years [17, 18]. Diosgenin is a naturally occurring steroidal sapogenin, with *Dioscorea zingiberensis* and *Dioscorea nipponica* being its two major natural sources. *Dioscorea nipponica* is used as the primary raw material for the commercial medicine "Di'ao Xinxuekang" [19-21]. Earlier studies have demonstrated that diosgenin exhibits numerous biological properties, including anti-inflammatory, antioxidant, and anticancer activities [22, 23]. Moreover, diosgenin has been shown to inhibit CRC cell proliferation and induce apoptosis [18, 24]. Nevertheless, whether diosgenin exerts its anti-CRC effects through regulation of the AKT1/IL-6/STAT3 signaling pathway remains unclear.

Based on the above findings, this study aimed to investigate whether diosgenin inhibits CRC cell proliferation, migration, and invasion and induces apoptosis through suppression of AKT1 phosphorylation, reduction of IL-6 secretion, and inhibition of the IL-6/STAT3 autocrine loop.

Materials and methods

Drugs and reagents

Diosgenin (purity ≥ 98%), temozolomide (TMZ), MK-2206, Stattic, and recombinant human IL-6 protein were purchased from Selleck Chemicals (USA). The CCK-8 kit was purchased from Dojindo (Japan). SYBR Green qPCR Master Mix was obtained from Takara (Japan). The human IL-6 ELISA kit was purchased from R&D Systems (USA).

The primary antibodies used in this study included antibodies against cleaved Caspase-3, P-AKT1 (Ser473), AKT1, Bax, P-STAT3 (Tyr705), STAT3, cleaved PARP, Bcl-2, IL-6, and actin, all of which were provided by Cell Signaling Technology (USA). HRP-labelled goat anti-rabbit and goat anti-mouse secondary reagents were obtained from Jackson ImmunoResearch (USA). Alexa Fluor 488- and 555-labelled fluorescent secondary antibodies were purchased from Invitrogen (USA).

Cell culture

The human CRC lines HCT116 and SW480 were procured from the ATCC(USA). HCT116 cells and SW480 cells were cultured in Dulbecco's modified Eagle's medium (DMEM) containing high glucose supplemented with 10% fetal bovine serum (FBS) and 1% penicillin/streptomycin (P/S). All cells were maintained at 37°C in a humidified atmosphere containing 5% CO_2.

CCK-8 experiment

HCT116 and SW480 cells were seeded into 96-well plates at a density of 5×10^3 cells/well, followed by the addition of 100 μL of complete culture medium. Following overnight attachment, cells were treated with increasing concentrations of diosgenin (0, 12.5, 25, 50, 75, 100, 150, 200 μM) for IC_{50} determination, or with diosgenin at 20, 40, and 60 μM for subsequent functional assays. TMZ was used at concentrations of 0, 50, 100, 200, 400, 600, 800, and 1000 μM. Three technical replicates were included for each concentration, and three independent biological experiments were performed. After 48 h of cultivation, cell viability was assessed using CCK-8 kit according to the manufacturer's instructions. Absorbance was measured at 450 nm using a microplate reader. Dose-response curves were plotted, and IC_{50} values were calculated using GraphPad Prism 10 software.

Transwell migration and invasion assays

Migration analysis: Cells were starved in serum-free medium for 12 h, trypsinized, and resuspended at a density of 2×10^5 cells/mL. Subsequently, 200 μL of cell suspension containing HCT116 cells (4×10^4 cells) or SW480 cells (2×10^4 cells), along with diosgenin (0, 20, 40, 60 μM), was added to the upper chamber of Transwell inserts. The lower chambers were filled with 600 μL of complete medium containing 10% FBS and the corresponding concentrations of diosgenin. To directly evaluate the effect of diosgenin on cell migratory ability rath-

er than FBS-induced chemotaxis, diosgenin was added to both the upper and lower chambers at equal concentrations to eliminate the drug-independent chemotactic gradient. After 24 h of incubation, non-migrating cells remaining on the upper membrane were gently wiped away, while migrating cells on the lower surface were fixed, stained with crystal violet, and counted in five randomly selected microscopic fields per well.

Invasion analysis: Matrigel was diluted 1:6 with serum-free liquid, and 50 μL of the diluted solution was evenly applied onto the upper surface of the Transwell membrane. The Matrigel was polymerized at 37°C for 2 h before use. Cells were seeded at density of 6×10^4 cells/well for HCT116 cells and 3×10^4 cells/well for SW480 cells. All subsequent procedures were the same as in the migration assay, except that the incubation period was extended to 48 h.

Flow cytometry analysis of apoptosis

HCT116 cells (5×10^5 per well) were cultured in 6-well plates and treated with vehicle (0.1% DMSO), diosgenin (20, 40, 60 μM), or TMZ (400 μM) for 48 h. Subsequently, cells were harvested and processed according to the manufacturer's instructions for the Annexin V-FITC apoptosis detection kit. Flow cytometry was used to evaluate the cell apoptosis status.

Western blot

Total cellular proteins were extracted from treated cells and quantified using a BCA assay. Equal amounts of protein samples were separated by SDS-PAGE and transferred onto PVDF membranes. The membranes were blocked with 5% non-fat milk for 1 h and incubated overnight at 4°C with primary antibodies, followed by incubation with HRP-conjugated secondary antibodies for 1 h. Protein bands were visualized using an ECL detection systems, and band intensities were quantified using ImageJ software.

ELISA

HCT116 cells were seeded into 6-well plates at a density of 2×10^5 cells per well. After overnight adhesion, the cells were exposed to diosgenin (0, 20, 40, 60 μM) or MK-2206 (5 μM) for 24 h. The culture supernatants were collected and centrifuged at 3,000 r/min for 10 min to remove cellular debris. IL-6 concentrations were determined using a commercial human IL-6 ELISA kit according to the manufacturer's instructions. Absorbance was measured at 450 nm, and IL-6 concentrations (pg/mL) were determined according to the provided standard curve.

qRT-PCR

Total RNA was extracted using TRIzol reagent after 24 h of treatment. RNA quality and concentration were assessed, followed by cDNA synthesis and qPCR with SYBR Green Master Mix. The primer sequences used were as follows: IL-6 forward, 5'-ACTCACCTCTTCAGAACGAATTG-3', reverse, 5'-CCATCTTTGGAAGGTTCAGGTTG-3'; GAPDH forward, 5'-GGAGCGAGATCCCTCCAAAAT-3', reverse, 5'-GGCTGTTGTCATACTTCTCATGG-3'. Relative IL-6 mRNA levels were calculated using the $2^{-\Delta\Delta Ct}$ method, with GAPDH used as the internal reference control.

AKT1 inhibitor (MK-2206) co-treatment experiment

HCT116 cells were divided into four groups: control group (0.1% DMSO), MK-2206 group (5 μM), diosgenin group (40 μM), and the combination treatment group (MK-2206 5 μM + diosgenin 40 μM). After 48 h of incubation, cell viability was assessed using the CCK-8 assay, cell migration was evaluated using Transwell assays, and the levels of P-AKT1, AKT1, P-STAT3, STAT3, and IL-6 were determined by Western blot.

AKT1 siRNA knockdown experiment

The siRNA sequences used in this study were as follows: si-AKT1#1 forward 5'-GAGCGACGUUGCCAUUGUATT-3'; si-AKT1#2 forward 5'-CCUGAAAGCUGCAAGAAUATT-3', negative control si-NC forward 5'-UUCUCCGAACGUGUCACGUdTdT-3'.

Knockdown efficiency validation: HCT116 cells were seeded into 6-well plates and then transfected with at approximately 60-70% confluence with 50 nM siRNA using Lipofectamine 3000. After 48 h of transfection, cells were collected, and AKT1 protein levels were assessed by Western blotting.

Functional assays: Cells were divided into four groups: si-NC, si-AKT1#2, si-NC + diosgenin (40 μM), and si-AKT1 #2 + diosgenin (40 μM). After 24 h of transfection, the culture medium was replaced with new fresh medium containing diosgenin, and cells were incubated for an additional 48 h. Subsequently, cell viability and migration ability were evaluated using CCK-8 and Transwell assays, respectively.

Exogenous IL-6 rescue experiment

HCT116 cells were divided into four groups: control group (0.1% DMSO), recombinant human IL-6 treatment group (20 ng/mL), diosgenin treatment group (40 μM), and combination treatment group (diosgenin, 40 μM + IL-6, 20 ng/mL). After 48 hours of incubation, cell viability was assessed using the CCK-8 assay, cell migration was evaluated by Transwell assay, and P-STAT3/STAT3 protein levels were determined by Western blot.

STAT3 inhibitor (Stattic) co-treatment experiment

HCT116 cells were assigned to four groups: control group (0.1% DMSO), Stattic treatment group (5 μM), diosgenin treatment group (40 μM), and combination treatment group (Stattic, 5 μM + diosgenin, 40 μM). After 48 h of incubation, cell viability was evaluated using the CCK-8 assay, and apoptosis was analyzed by Annexin V-FITC/PI flow cytometry.

Immunofluorescence assay

Immunofluorescence staining was performed following standard procedures. Briefly, after treatment with vehicle or 40 μM diosgenin for 48 h, HCT116 cells were fixed, permeabilized, and blocked. Cells were then incubated with primary antibodies against P-AKT1 and P-STAT3 overnight at 4°C, followed by incubation with corresponding fluorescent secondary antibodies. Nuclei were counterstained with DAPI. Images were acquired using a confocal microscope, and fluorescence intensity and the nuclear/cytoplasmic ratio were quantified using ImageJ software. The nuclear/cytoplasmic fluorescence intensity ratio of each treatment group was normalized to that of the control group.

Statistical analysis

Statistical analyses were performed using GraphPad Prism 10 software. All experiments were performed using three independent biological replicates, and data were presented as mean ± standard deviation (SD). Differences between the two groups were assessed using a two-tailed Student's t-test. For comparisons among multiple groups, one-way ANOVA followed by Dunnett's or Tukey's post-hoc test was performed, as appropriate. A two-sided *P*-value < 0.05 was considered statistically significant. Statistical significance in figures is indicated as follows: $^{*}P < 0.05$, $^{**}P < 0.01$, $^{***}P < 0.001$, and $^{****}P < 0.0001$.

Results

Diosgenin inhibits proliferation, migration and invasion of colorectal cancer cells

To investigate the in vitro anti-cancer effects of diosgenin on CRC cells, the CCK-8 assay was initially used to determine its effect on the viability of HCT116 and SW480 cells. As shown in **Figure 1A**, **1B**, after 48 h of treatment with 60 μM diosgenin, the viability of HCT116 and SW480 cells decreased to 38.5 ± 4.5% and 58.2 ± 5.0%, respectively. In contrast, TMZ at the same dose, used as a reference drug, did not significantly affect the viability of either cell line (> 95%). Dose-response plots (**Figure 1C**, **1D**) demonstrated that diosgenin inhibited cell survival in a concentration-dependent manner, with IC_{50} values of 51.81 ± 2.5 μM and 73.53 ± 3.2 μM for HCT116 cells and SW480 cells, respectively. By comparison, the IC_{50} values of TMZ in HCT116 and SW480 cells were approximately 706.9 ± 35.1 μM and 432.9 ± 24.3 μM, respectively, indicating that diosgenin exhibited stronger cytotoxic effects than TMZ under the experimental conditions.

The effects of diosgenin on CRC cell migration and invasion were also examined using Transwell assays. As shown in **Figure 1E-I**, incubation with diosgenin for 24 h (migration) and 48 h (invasion) significantly reduced the numbers of migrating and invading HCT116 and SW480 cells in a dose-dependent manner compared with the control group. At 60 μM, diosgenin inhibited HCT116 cell migration and invasion by 70.2 ± 4.5% and 71.4 ± 5.2%, respectively (**Figure 1F**, **1H**); the corresponding inhibition rates for SW480 cells were approximately 55 ± 4.8% and 57 ± 5.0%, respectively (**Figure 1G**, **1I**). These findings demonstrate that diosgenin effectively suppresses the migratory and invasive abilities of CRC cells.

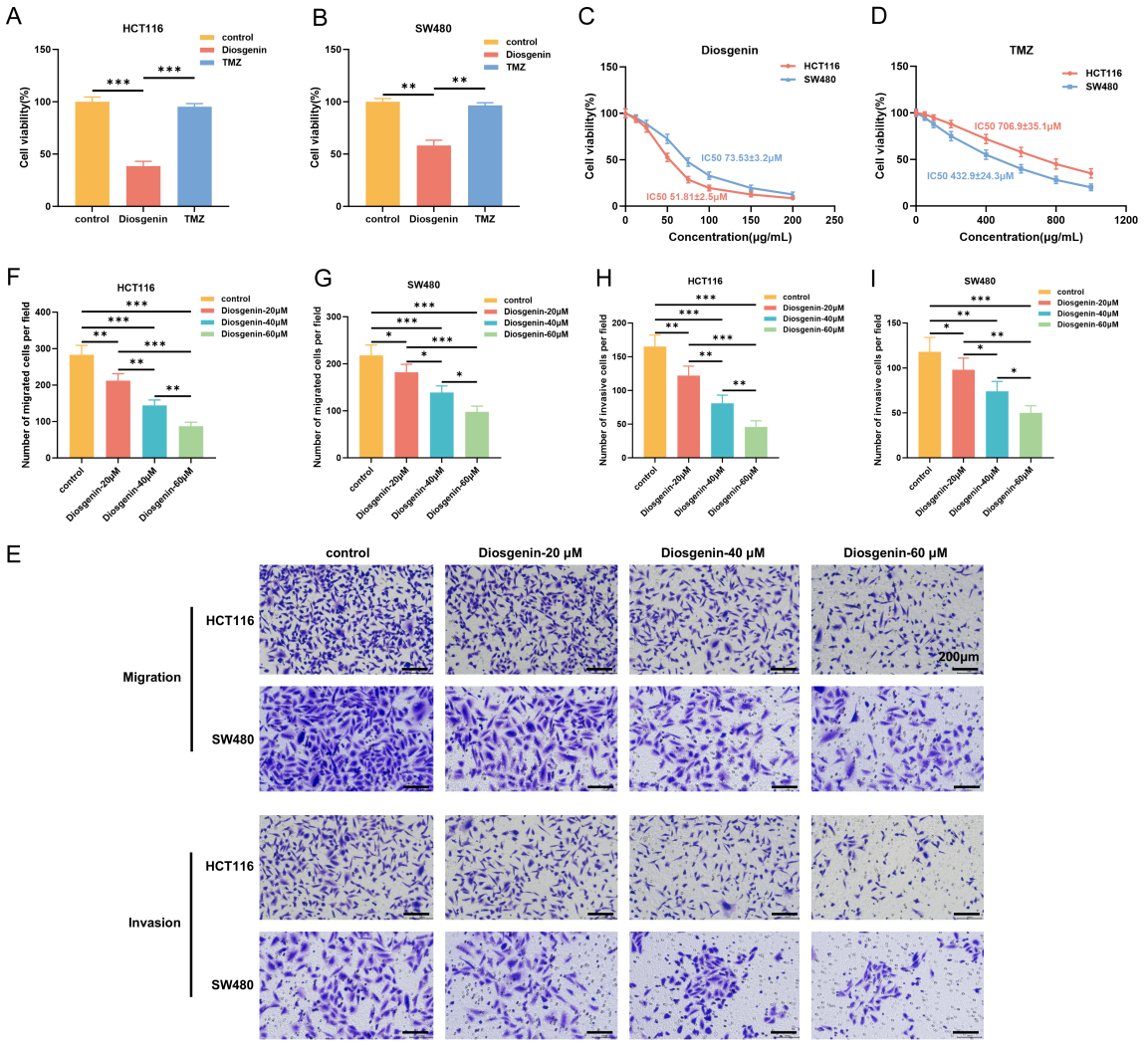


Figure 1. Diosgenin inhibits proliferation, migration and invasion in colorectal cancer cells. (A, B) Bar graphs of the viability of HCT116 (A) and SW480 (B) cells after 48 h of exposure to diosgenin or TMZ. (C, D) Dose-response plots for HCT116 (C) and SW480 (D) cells incubated with diosgenin for 48 h. (E) Typical crystal violet staining images of Transwell migration and invasion assays; scale bar = 200 μm. (F-I) Quantitative analysis of migrated (F, G) and invaded (H, I) cells. Notes: $^{*}P < 0.05$, $^{**}P < 0.01$, and $^{***}P < 0.001$.

Diosgenin induces apoptosis in colorectal cancer cells

To investigate the mechanism underlying diosgenin-induced reduction in cell viability, apoptosis was analyzed using Annexin V-FITC/PI double staining flow cytometry. Diosgenin treatment for 48 h increased the proportion of apoptotic HCT116 cells in a dose-dependent manner (**Figure 2A**, **2B**). The apoptosis rates were 9.9 ± 1.6%, 22.7 ± 2.8% and 38.4 ± 3.5% in the 20, 40 and 60 μM diosgenin groups, respectively, compared with 3.2 ± 0.7% in the control group. TMZ (400 μM) as a reference drug induced a total apoptosis rate of 16.0 ± 2.2%. WB analysis (**Figure 2C-G**) further showed that diosgenin treatment increased the expression levels of cleaved Caspase-3, cleaved PARP and Bax, while decreasing Bcl-2 expression.

Diosgenin inhibits the AKT1/IL-6/STAT3 signaling pathway

WB analysis (**Figure 3A-C**) showed that diosgenin treatment for 48 h decreased the P-AKT1/AKT1 and P-STAT3/STAT3 ratios in HCT116 cells in a concentration-dependent manner. In addition, the specific AKT1 inhibitor MK-2206 significantly suppressed the phosphorylation of AKT1 and STAT3. ELISA results (**Figure 3D**)

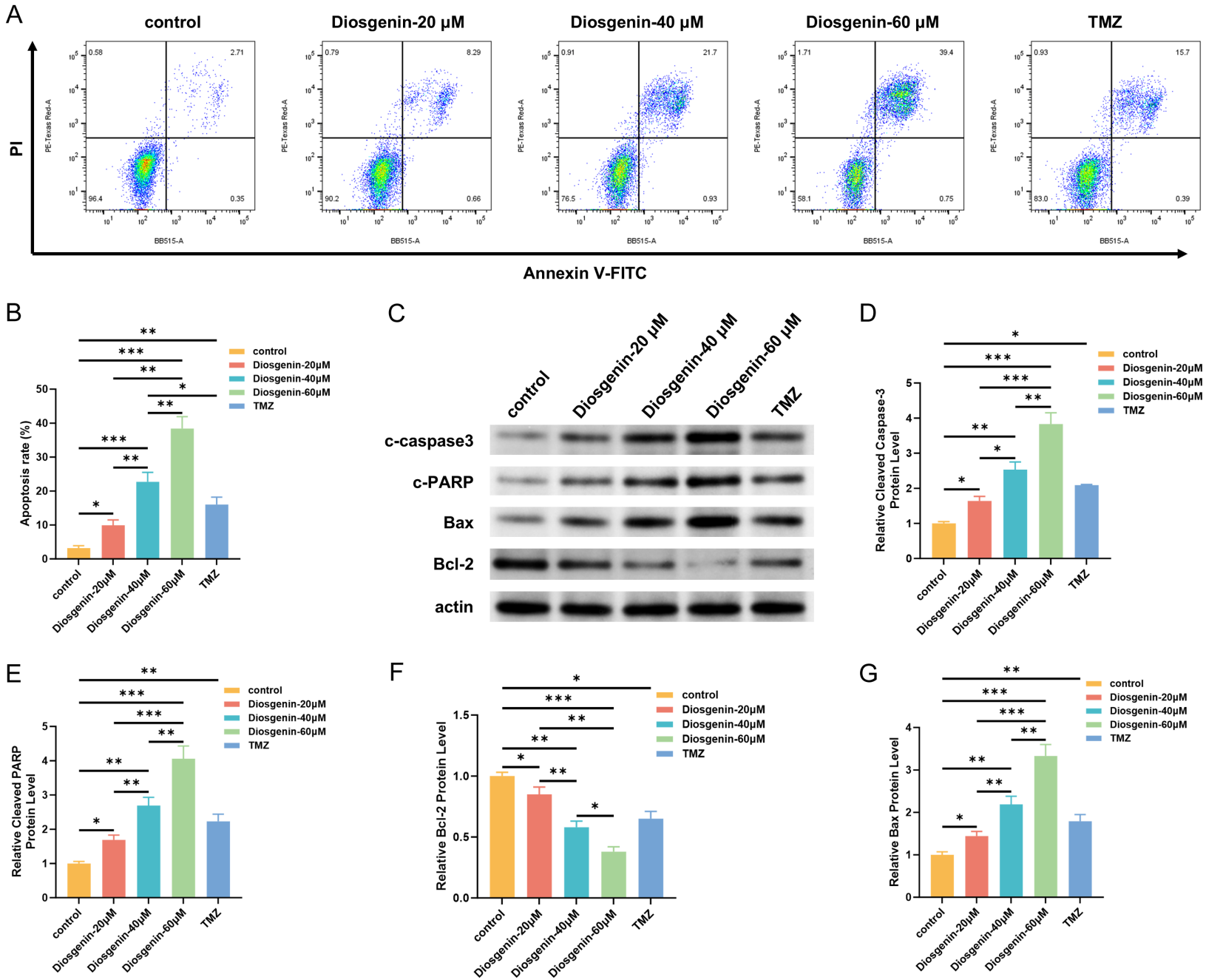

A
control
Diosgenin-20 μM
Diosgenin-40 μM
Diosgenin-60 μM
TMZ
PI
Annexin V-FITC
PE-Texas Red-A
BB515-A
0.58
2.71
96.4
0.35
0.79
8.29
90.2
0.66
0.91
21.7
76.5
0.93
1.71
39.4
58.1
0.75
0.93
15.7
83.0
0.39
B
Apoptosis rate (%)
control
Diosgenin-20μM
Diosgenin-40μM
Diosgenin-60μM
TMZ
C
control
Diosgenin-20 μM
Diosgenin-40 μM
Diosgenin-60 μM
TMZ
c-caspase3
c-PARP
Bax
Bcl-2
actin
D
Relative Cleaved Caspase-3 Protein Level
E
Relative Cleaved PARP Protein Level
F
Relative Bcl-2 Protein Level
G
Relative Bax Protein Level

Figure 2. Diosgenin induces apoptosis in HCT116 cells. A. Representative dot plots obtained from Annexin V-FITC/PI flow cytometry analysis. B. Quantification of the total apoptotic cell population. C. Representative Western blotting images showing the protein expression levels of cleaved Caspase-3, cleaved PARP, Bax, Bcl-2 and actin. D-G. Quantitative analysis of normalized protein levels. Notes: $^{*}P < 0.05$, $^{**}P < 0.01$, and $^{***}P < 0.001$.

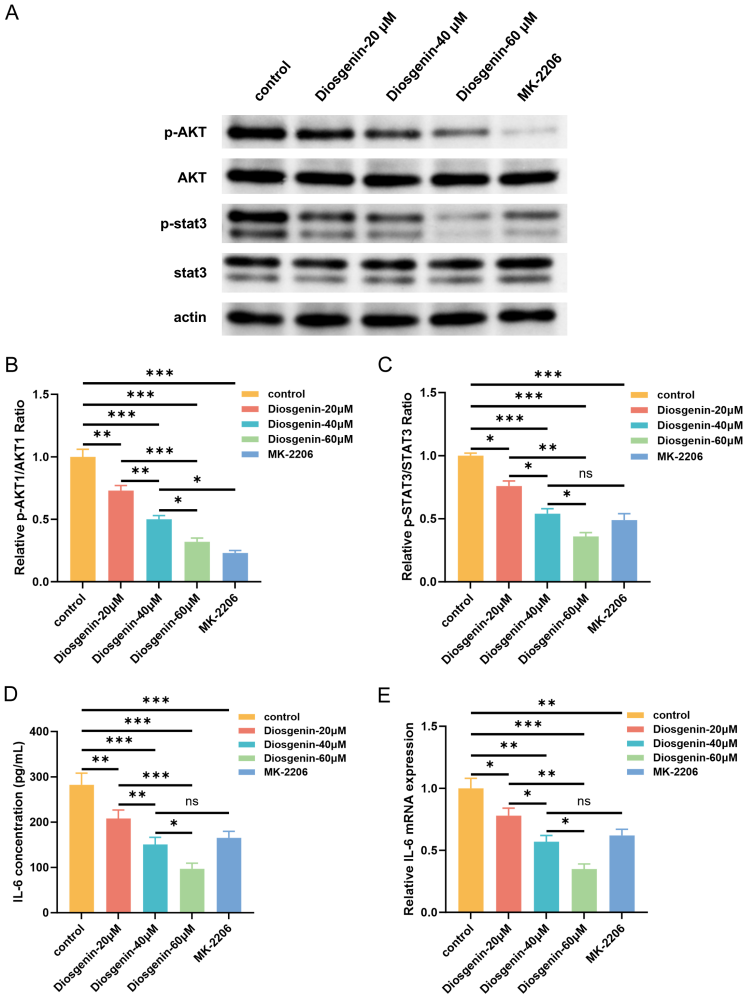


Figure 3. Diosgenin inhibits the AKT1/IL-6/STAT3 signaling pathway in HCT116 cells. A. Western blot analysis of P-AKT1, AKT1, P-STAT3, STAT3, and actin. B, C. Bar graphs of the ratios P-AKT1/AKT1 and P-STAT3/STAT3. D. ELISA experiments to quantify IL-6 in cell culture medium. E. qRT-PCR results of IL-6 mRNA relative expression. Notes: ns, not significant, $^{*}P < 0.05$, $^{**}P < 0.01$, and $^{***}P < 0.001$.

showed that diosgenin decreased IL-6 secretion in a concentration-dependent manner. The IL-6 concentration in the control group (0 μM) was 282.5 ± 25.5 pg/mL, and the concentrations in the 20, 40 and 60 μM diosgenin treatment groups were 208.2 ± 18.5, 151.0 ± 15.5, and 97.0 ± 12.5 pg/mL, respectively. MK-2206 (5 μM) also significantly reduced IL-6 secretion to 165.2 ± 14.5 pg/mL. qRT-PCR analysis (**Figure 3E**) further demonstrated that diosgenin inhibited IL-6 mRNA expression, suggesting regulation at the transcriptional level. Collectively, these findings indicate that diosgenin inhibits AKT1 phosphorylation, reduces IL-6 production, and consequently suppresses STAT3 activation.

AKT1 is a key target of diosgenin in suppressing colorectal cancer

To determine whether AKT1 mediates the anticancer effects of diosgenin, functional rescue experiments were performed using the AKT1 inhibitor MK-2206 and AKT1-specific siRNA. As shown in **Figure 4A-C**, MK-2206 alone reduced cell viability to 70.8 ± 3.7% and decreased the number of migrating cells to 185 ± 18 cells/field. Diosgenin alone reduced cell viability to 77.1 ± 4.1% and migration counts to 147 ± 11 cells/field. Combined treatment with MK-2206 and diosgenin further decreased cell viability to 46.2 ± 3.6% and migration counts to 83 ± 10 cells/field, indicating an enhanced inhibitory effect compared with either treatment alone. WB analysis (**Figure 4D-G**) showed that the P-AKT1/AKT1 and P-STAT3/STAT3 ratios, as well as IL-6 protein levels, were all significantly lower in the combination group compared to the single-agent group.

To further validate the role of AKT1, two siRNAs were used to silence AKT1 expression. si-AKT1#2 achieved a higher knockdown efficiency (around 75%; **Figure 4H**, **4I**) and was selected for subsequent experiments. AKT1 knockdown alone partially reduced cell viability and

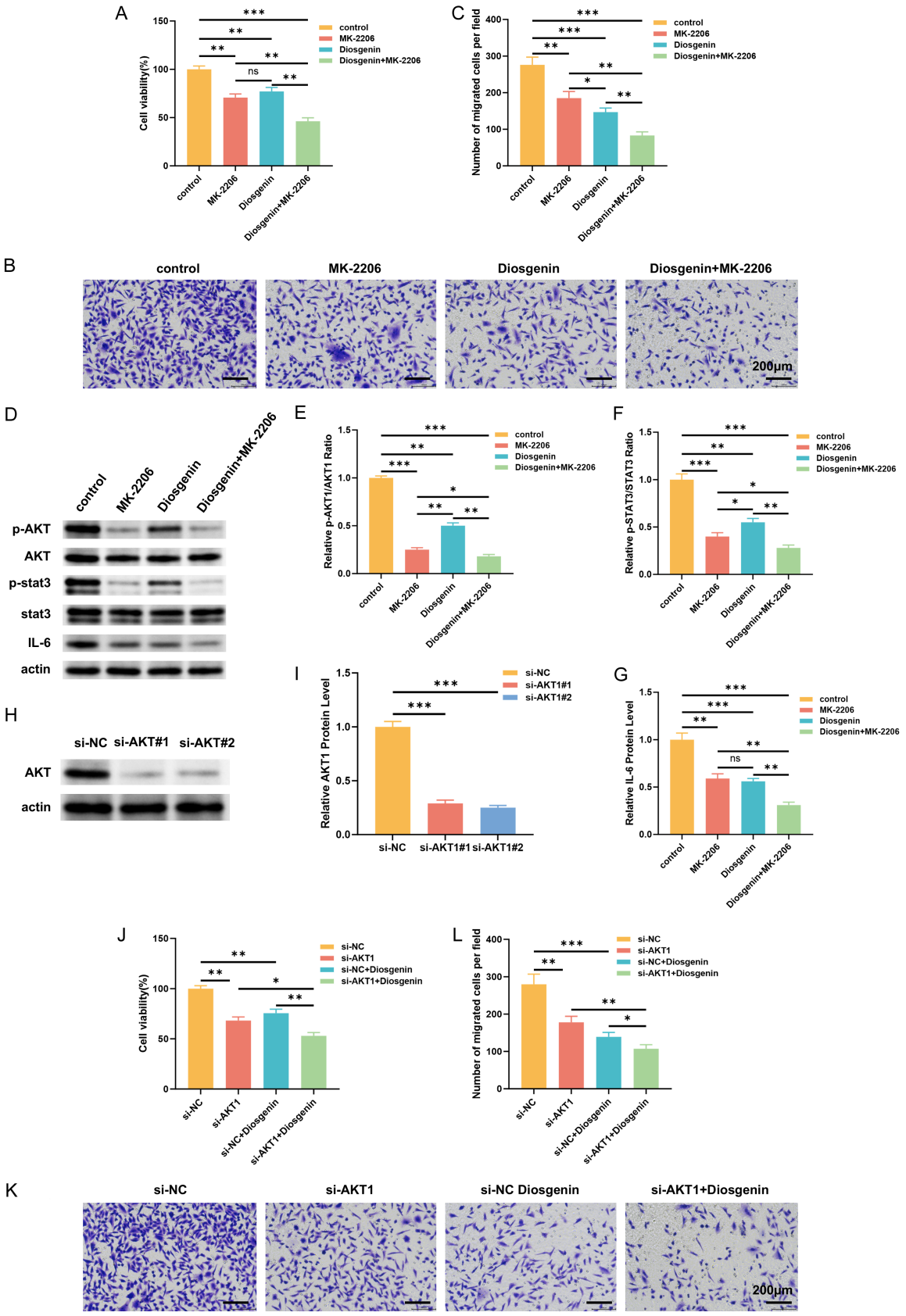


Figure 4. AKT1 signaling contributes to the inhibitory effects of diosgenin on colorectal cancer cells. (A) Quantification of cell viability after MK-2206 co- treatment using CCK-8 assay. (B, C) Representative crystal violet staining

photos (B) and quantitative analysis (C) of Transwell migration assays after MK-2206 co-treatment; scale bar = 200 μm. (D-G) Representative Western blot images (D) and quantitative analysis (E-G) of P-AKT1, AKT1, P-STAT3, STAT3, IL-6 and actin expression after MK-2206 co-treatment. (H, I) Representative Western blot images (H) and quantitative analysis (I) of AKT1 silencing efficiency. (J) Quantification of cell viability after AKT1 siRNA transfection using the CCK-8 assay. (K, L) Representative crystal violet staining photos (K) and quantitative analysis (L) of Transwell migration assays after AKT1 siRNA silencing; scale bar = 200 μm. Notes: ns, not significant, $^{*}P < 0.05$, $^{**}P < 0.01$ and $^{***}P < 0.001$.

migration; In the presence of si-NC, diosgenin treatment decreased cell viability to 75.5 ± 4.1% and reduced migration to 139 ± 12 cells/field. Notably, combined treatment of si-AKT and diosgenin synergistically decreased cell viability and migration (**Figure 4J-L**). These findings suggest that AKT1 is involved in, and may contribute to, the anticancer effects of diosgenin in colorectal cancer cells.

Diosgenin exerts anti-tumor effects via the IL-6/STAT3 axis

To further validate the involvement of the IL-6/STAT3 axis in the anti-tumor effects of diosgenin, rescue experiments with exogenous IL-6 supplementation and co-treatment with the STAT3 inhibitor Stattic were performed. As shown in **Figure 5A-E**, recombinant human IL-6 treatment alone increased cell viability, migration and P-STAT3 expression, whereas diosgenin treatment significantly reduced these indicators. Importantly, exogenous IL-6 partially restored the inhibitory effects of diosgenin on cell viability, migration, and STAT3 activation.

Moreover, co-treatment of Stattic with diosgenin exhibited a synergistic effect. As shown in **Figure 5F-H**, the combined treatment further decreased cell viability to 42.2 ± 3.2% and increased total apoptotic rate to 47.5 ± 4.0%, both of which were substantially better than in the single-drug treatment group. These findings indicate that the IL-6/STAT3 signaling pathway contributes to the inhibitory effects of diosgenin on colorectal cancer cells.

Diosgenin reduces nuclear translocation of P-AKT1 and P-STAT3

Immunofluorescence staining was performed to further examine the effects of diosgenin on the subcellular localization of P-AKT1 and P-STAT3. As shown in **Figure 6A**, in the control group, P-AKT1 (green) and P-STAT3 (red) fluorescent signals were strongly detected in both the cytoplasm and the nucleus, with evident nuclear accumulation. The merged images showed extensive yellow fluorescence.

After diosgenin treatment for 48 h, the fluorescence intensity of P-AKT1 and P-STAT3 was significantly reduced (**Figure 6B**), nearly all nuclear staining disappeared, and only faint diffuse signals remained in the cytosol. Quantitative analysis of the nuclear/cytoplasmic fluorescence intensity ratio (**Figure 6C**) showed that diosgenin treatment reduced the nuclear/cytoplasmic ratio of P-AKT1 and P-STAT3 from 1.00 ± 0.10 to 0.45 ± 0.06 and 0.50 ± 0.07, respectively. These findings suggest that diosgenin suppresses the nuclear translocation of P-AKT1 and P-STAT3. Consistent with the WB results, these data indicate that diosgenin effectively inhibits both the activation and nuclear translocation of AKT1 and STAT3 signaling.

Discussion

Colorectal cancer is a major digestive system malignancy with high incidence and mortality rates worldwide [1, 25, 26]. Although comprehensive treatment strategies have continuously advanced, the prognosis of patients with advanced and metastatic CRC remains poor [27, 28]. In the present study, we demonstrated that diosgenin inhibited CRC cell viability, migration and invasion in a concentration-dependent manner, induced mitochondrial apoptosis, and decreased the nuclear translocation of P-AKT1 and P-STAT3 by suppressing the AKT1/IL-6/STAT3 signaling axis.

The AKT signaling pathway plays an important role in CRC progression, and its aberrant activation promotes tumor growth, metastasis, and resistance to chemotherapy [29]. In this study, diosgenin significantly reduced AKT1 phosphorylation, and pharmacological inhibition of AKT1 with MK-2206 or genetic AKT1 knockdown further enhanced the inhibitory effects of diosgenin on CRC cell viability and migration. These findings are consistent with previous studies reporting that natural products can

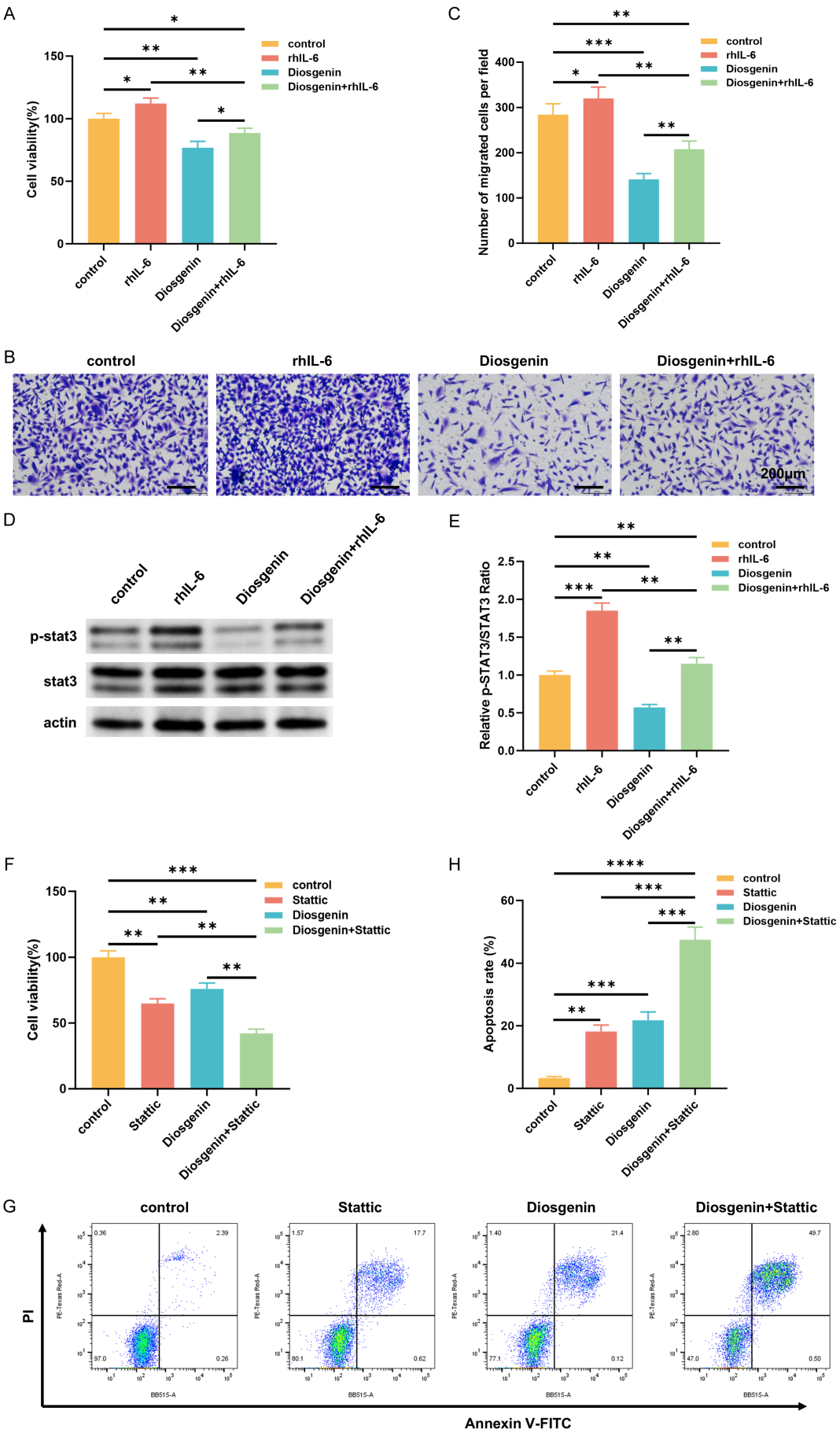

A
Cell viability(%)
control
rhIL-6
Diosgenin
Diosgenin+rhIL-6
C
Number of migrated cells per field
B
control
rhIL-6
Diosgenin
Diosgenin+rhIL-6
200μm
D
p-stat3
stat3
actin
E
Relative p-STAT3/STAT3 Ratio
F
Cell viability(%)
Stattic
Diosgenin+Stattic
H
Apoptosis rate (%)
G
PI
Annexin V-FITC

Figure 5. Diosgenin exerts anti-cancer effects through modulation of the IL-6/STAT3 signaling pathway. (A) Quantification of cell viability assessed by the CCK-8 assay in the exogenous IL-6 rescue experiment. (B, C) Representative crystal violet staining images (B) and quantitative analysis (C) of Transwell migration assays following exogenous IL-6 supplementation; scale bar = 200 μm. (D, E) Representative Western blot images (D) and semi-quantitative analysis (E) of P-STAT3, STAT3, and actin expression in the exogenous IL-6 rescue study. (F) Quantification of cell viability assessed by CCK-8 assay in the Stattic co-treatment experiment. (G, H) Representative dot plots (G) and quantitative analysis (H) of total apoptotic cell populations detected by Annexin V-FITC/PI flow cytometry following Stattic co-treatment. Notes: $^{*}P < 0.05$, $^{**}P < 0.01$ and $^{***}P < 0.001$.

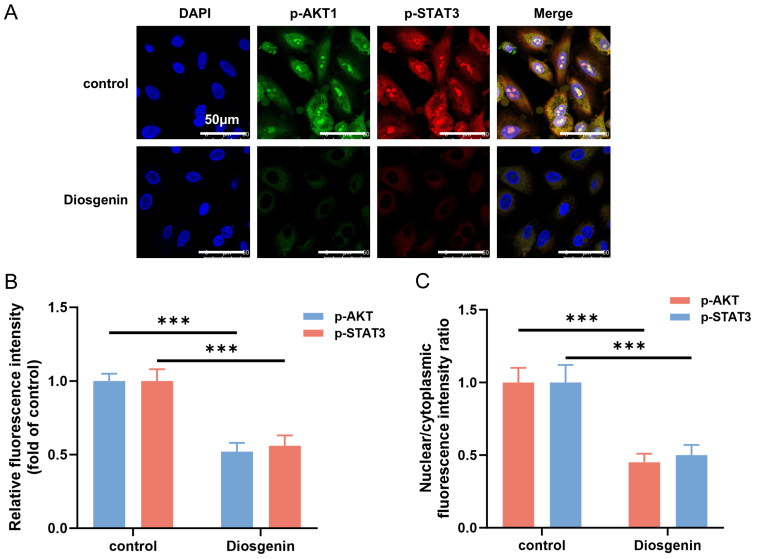


Figure 6. Diosgenin inhibits the nuclear translocation of P-AKT1 and P-STAT3. A. Representative immunofluorescence images: DAPI (blue), P-AKT1 (green), P-STAT3 (red) and combined, scale bar = 50 μm. B. Quantitative analysis of the average fluorescence intensity of P-AKT1 and P-STAT3. C. Quantitative analysis of the nuclear/cytoplasmic fluorescence intensity ratios of P-AKT1 and P-STAT3. The nuclear/cytoplasmic ratios were normalized to the control group. Note: $^{***}P < 0.001$.

inhibit CRC progression by regulating the AKT signaling pathway [30]. In addition, AKT signaling has been reported to contribute to cancer stem cell self-renewal and chemoresistance in hepatocellular carcinoma and glioblastoma [31]. As a natural steroidal sapogenin, diosgenin may possess advantages over conventional AKT inhibitors due to its multiple biological activities and potentially lower toxicity. Similar advantages have been observed in other bioactive materials derived from traditional Chinese medicine, such as tanshinone [32, 33].

Persistent activation of the IL-6/STAT3 signaling axis is a major driver of malignant phenotypes in CRC [34]. Our findings showed that diosgenin inhibited the expression of IL-6 at both the mRNA and protein levels and suppressed STAT3 activation. External IL-6 supplementation partially reversed the anti-tumor effects of diosgenin, supporting the involvement of the IL-6/STAT3 pathway in the anticancer activity of diosgenin. These results are consistent with previous studies reporting that AKT signaling can promote tumor progression by regulating the IL-6 autocrine cycle in gliomas and non-small cell lung cancers [35, 36]. Similarly, inhibition of the IL-6/STAT3 pathway has been shown to suppress malignant cell growth in prostate cancer and other solid tumors [37]. However, the novelty of our work lies in demonstrating that diosgenin regulates the AKT1/IL-6/STAT3 signaling network in CRC cells, affecting both upstream AKT1 activation and downstream STAT3 signaling.

The combined treatment with the STAT3 inhibitor Stattic and diosgenin further enhanced the inhibitory effects, highlighting the potential therapeutic relevance of targeting the IL-6/STAT3 pathway in CRC treatment. Combination therapy significantly reduced cell viability and increased apoptosis compared with either treatment alone; suggesting that co-inhibition of AKT1 and STAT3 may provide enhanced anti-tumor effect. This concept is in line with the emerging therapeutic strategy of “dual-target” or “multi-target” intervention [38]. Within the tumor microenvironment, IL-6 is produced not only by cancer cells but also by cancer-associated fibroblasts and macrophages [39]. Therefore, diosgenin-mediated reduction of IL-6 secretion may potentially influence the inflammatory characteristics of the tumor microenvironment, which warrants further investigation.

Several limitations of this study need to be acknowledged. First, all experiments were per-

formed using in vitro cell systems, and in vivo validation in animal models was not performed. Although our findings demonstrate that diosgenin modulates the AKT1/IL-6/STAT3 signaling pathway in CRC cells, whether these molecular effects translate into therapeutic benefits within the complex tumor microenvironment in vivo remains unclear. Second, the use of temozolomide (TMZ) as a reference drug is a limitation of this study. TMZ is primarily used for the treatment of glioma and is not a standard chemotherapeutic agent for CRC. The observed relatively limited inhibitory effect of TMZ on HCT116 and SW480 cells is consistent with previous studies reporting its limited activity in CRC models, potentially due to MGMT expression and mismatch repair (MMR) status. Although TMZ was included as a comparator to evaluate the relative anticancer activity of diosgenin, clinically relevant CRC therapeutic agents, such as 5-fluorouracil, oxaliplatin, or irinotecan, would provide more appropriate reference controls. Future studies will employ these drugs to further validate the anti-CRC activity of diosgenin.

Third, although both pharmacological inhibition (MK-2206) and genetic knockdown (siRNA) approaches were used to investigate the involvement of AKT1, an AKT1 overexpression rescue experiment-such as transfection with constitutively active AKT1-would further strengthen the causal relationship between AKT1 inhibition and diosgenin-mediated regulation of the IL-6/STAT3 pathway. Fourth, the Transwell experimental design, in which diosgenin was added to both the upper and lower chambers, does not fully distinguish between effects on chemotaxis and intrinsic cell motility. Therefore, our conclusion is limited to the observation that diosgenin suppresses overall migration through modulation of the AKT1/IL-6/STAT3 signaling pathway. Future studies employing a modified Transwell system (with drug only in the upper chamber) are required to separately evaluate the effects of diosgenin on chemotactic responses and cell motility.

Fifth, the current monoculture cell model only addresses the autocrine IL-6/STAT3 loop and doesn't account for paracrine IL-6 production from components of the tumor microenvironment, such as cancer-associated fibroblasts and macrophages. Future investigations using co-culture systems or stromal cell-derived conditioned media are needed to evaluate the contribution of paracrine IL-6/STAT3 axis to CRC progression. Finally, the poor water solubility and limited pharmacokinetic properties of diosgenin may restrict its in vivo bioavailability and therapeutic application. Although research on nanocarriers has shown potential for improving diosgenin absorption, further pharmacokinetic/pharmacodynamic (PK/PD) studies are required. In addition, this study did not investigate upstream regulators of AKT1, such as PI3K and PTEN, nor did it determine whether diosgenin directly interacts with AKT1 protein. Future studies incorporating molecular docking, surface plasmon resonance, and CRC xenograft models are warranted.

Conclusion

This study provides evidence that diosgenin inhibits CRC cell proliferation, migration and invasion and induces apoptosis by modulating the AKT1/IL-6/STAT3 signaling axis. These findings suggest that diosgenin represents a potential bioactive component. Further in vivo studies using animal models are warranted to validate its therapeutic efficacy, clarify its pharmacological mechanisms, and evaluate its potential for future clinical translation.

Disclosure of conflict of interest

None.

Address correspondence to: Yumo Yuan, School of Elderly Care Services and Management, Nanjing University of Chinese Medicine, No. 138 Xianlin Avenue, Qixia District, Nanjing 210023, Jiangsu, China. E-mail: 19975011230@163.com

References

[1] Siegel RL, Giaquinto AN and Jemal A. Cancer statistics, 2024. CA Cancer J Clin 2024; 74: 12-49.

[2] Wu S, Zhang Y, Lin Z and Wei M. Global burden of colorectal cancer in 2022 and projections to 2050: incidence and mortality estimates from GLOBOCAN. BMC Cancer 2025; 25: 1770.

[3] Bray F, Laversanne M, Sung H, Ferlay J, Siegel RL, Soerjomataram I and Jemal A. Global cancer statistics 2022: GLOBOCAN estimates of incidence and mortality worldwide for 36 cancers in 185 countries. CA Cancer J Clin 2024; 74: 229-263.

[4] Turri G, Ostuzzi G, Vita G, Barresi V, Scarpa A, Milella M, Mazzarotto R, Ruzzenente A, Barbui C and Pedrazzani C. Treatment of locally advanced rectal cancer in the era of total neoadjuvant therapy: a systematic review and network meta-analysis. JAMA Netw Open 2024; 7: e2414702.
[5] Zhou YJ, Tan ZE, Zhuang WD and Xu XH. Analysis of cancer-specific survival in patients with metastatic colorectal cancer: a evidence-based medicine study. World J Gastrointest Surg 2024; 16: 1791-1802.
[6] Manning BD and Toker A. AKT/PKB signaling: navigating the network. Cell 2017; 169: 381-405.
[7] Hinz N and Jücker M. Distinct functions of AKT isoforms in breast cancer: a comprehensive review. Cell Commun Signal 2019; 17: 154.
[8] Yaeger R, Chatila WK, Lipsyc MD, Hechtman JF, Cercek A, Sanchez-Vega F, Jayakumaran G, Middha S, Zehir A, Donoghue MTA, You D, Viale A, Kemeny N, Segal NH, Stadler ZK, Varghese AM, Kundra R, Gao J, Syed A, Hyman DM, Vakiani E, Rosen N, Taylor BS, Ladanyi M, Berger MF, Solit DB, Shia J, Saltz L and Schultz N. Clinical sequencing defines the genomic landscape of metastatic colorectal cancer. Cancer Cell 2018; 33: 125-136, e123.
[9] Li Q, Geng S, Luo H, Wang W, Mo YQ, Luo Q, Wang L, Song GB, Sheng JP and Xu B. Signaling pathways involved in colorectal cancer: pathogenesis and targeted therapy. Signal Transduct Target Ther 2024; 9: 266.
[10] Johnson DE, O'Keefe RA and Grandis JR. Targeting the IL-6/JAK/STAT3 signalling axis in cancer. Nat Rev Clin Oncol 2018; 15: 234-248.
[11] Waldner MJ, Foersch S and Neurath MF. Interleukin-6--a key regulator of colorectal cancer development. Int J Biol Sci 2012; 8: 1248-1253.
[12] Taniguchi K and Karin M. IL-6 and related cytokines as the critical lynchpins between inflammation and cancer. Semin Immunol 2014; 26: 54-74.
[13] He G and Karin M. NF-κB and STAT3 - key players in liver inflammation and cancer. Cell Res 2011; 21: 159-168.
[14] Chen HY, Lin LT, Wang ML, Lee SH, Tsai ML, Tsai CC, Liu WH, Chen TC, Yang YP, Lee YY, Chang YL, Huang PI, Chen YW, Lo WL, Chiou SH and Chen MT. Musashi-1 regulates AKT-derived IL-6 autocrinal/paracrinal malignancy and chemoresistance in glioblastoma. Oncotarget 2016; 7: 42485-42501.
[15] Malanga D, De Marco C, Guerriero I, Colelli F, Rinaldo N, Scrima M, Mirante T, De Vitis C, Zoppoli P, Ceccarelli M, Riccardi M, Ravo M, Weisz A, Federico A, Franco R, Rocco G, Mancini R, Rizzuto A, Gulletta E, Ciliberto G and Viglietto G. The Akt1/IL-6/STAT3 pathway regulates growth of lung tumor initiating cells. Oncotarget 2015; 6: 42667-42686.
[16] Li X, Zhao Z, Ye H, Li D, Huang X, Lee JH and Liu R. CD01 phosphorylation is required for IL-6-induced tumor cell proliferation through governing cysteine availability. Cell Commun Signal 2025; 23: 194.
[17] Li S, Chen X, Shi H, Yi M, Xiong B and Li T. Tailoring traditional Chinese medicine in cancer therapy. Mol Cancer 2025; 24: 27.
[18] Kumar A, Amita, Singh B, Sharma P, Raina R, Sharma B, Haque S and Tuli HS. Role of diosgenin in gastrointestinal cancers: recent trends and future perspectives. Med Oncol 2025; 42: 397.
[19] Zhang S, Li L, Deng M, Wang Y, Shen A and Zhang L. Di'ao Xinxuekang: therapeutic potential in cardiovascular diseases. Curr Mol Pharmacol 2021; 14: 975-985.
[20] Kang TH, Moon E, Hong BN, Choi SZ, Son M, Park JH and Kim SY. Diosgenin from Dioscorea nipponica ameliorates diabetic neuropathy by inducing nerve growth factor. Biol Pharm Bull 2011; 34: 1493-1498.
[21] Zhang Y, Tang L, An X, Fu E and Ma C. Modification of cellulase and its application to extraction of diosgenin from Dioscorea zingiberensis CH Wright. Biochem Eng J 2009; 47: 80-86.
[22] Semwal P, Painuli S, Abu-Izneid T, Rauf A, Sharma A, Daştan SD, Kumar M, Alshehri MM, Taheri Y, Das R, Mitra S, Emran TB, Sharifi-Rad J, Calina D and Cho WC. Diosgenin: an updated pharmacological review and therapeutic perspectives. Oxid Med Cell Longev 2022; 2022: 1035441.
[23] Karami-Mohajeri S, Mohammadinejad R, Ashrafizadeh M, Mohamadi N, Mohajeri M and Sharififar F. Diosgenin: mechanistic insights on its anti-inflammatory effects. Antiinflamm Antiallergy Agents Med Chem 2022; 21: 2-9.
[24] Lai Z, Wang H, Tang X, Zhang L, Wang T and Cheng J. Study on the mechanism of diosgenin targeting STAT3 to inhibit colon cancer proliferation and migration. Dis Markers 2022; 2022: 7494887.
[25] Candia L, Cervantes A and Martinelli E; ESMO Guidelines Committee. Updated treatment recommendations for third and further lines of treatment in advanced colorectal cancer: from the ESMO Metastatic Colorectal Cancer Living Guideline. Ann Oncol 2025; 36: 342-344.
[26] Huo Z, Liu G and Li J. Recent research progress and clinical status of immunotherapy for colorectal cancer. J Adv Res 2026; 82: 729-750.
[27] Lee HO, Hong Y, Etlioglu HE, Cho YB, Pomella V, Van den Bosch B, Vanhecke J, Verbandt S,

Hong H, Min JW, Kim N, Eum HH, Qian J, Boeckx B, Lambrechts D, Tsantoulis P, De Hertogh G, Chung W, Lee T, An M, Shin HT, Joung JG, Jung MH, Ko G, Wirapati P, Kim SH, Kim HC, Yun SH, Tan IBH, Ranjan B, Lee WY, Kim TY, Choi JK, Kim YJ, Prabhakar S, Tejpar S and Park WY. Lineage-dependent gene expression programs influence the immune landscape of colorectal cancer. Nat Genet 2020; 52: 594-603.

[28] Parikh AR, Szabolcs A, Allen JN, Clark JW, Wo JY, Raabe M, Thel H, Hoyos D, Mehta A, Arshad S, Lieb DJ, Drapek LC, Blaszkowsky LS, Giantonio BJ, Weekes CD, Zhu AX, Goyal L, Nipp RD, Dubois JS, Van Seventer EE, Foreman BE, Matlack LE, Ly L, Meurer JA, Hacohen N, Ryan DP, Yeap BY, Corcoran RB, Greenbaum BD, Ting DT and Hong TS. Radiation therapy enhances immunotherapy response in microsatellite stable colorectal and pancreatic adenocarcinoma in a phase II trial. Nat Cancer 2021; 2: 1124-1135.

[29] Leiphrakpam PD and Are C. PI3K/Akt/mTOR signaling pathway as a target for colorectal cancer treatment. Int J Mol Sci 2024; 25: 3178.

[30] Zhang Y, Luo H, Ma P, Leng Y, Tan Y, Zhuo S, Tan C and Xu D. Androsin alleviates colorectal cancer by inhibiting the PI3K/Akt-centered signaling pathway. Korean J Physiol Pharmacol 2026; 30: 155-168.

[31] Rivas S, Gómez-Oro C, Antón IM and Wandosell F. Role of Akt isoforms controlling cancer stem cell survival, phenotype and self-renewal. Biomedicines 2018; 6: 29.

[32] Chen F, Xiang W and Qiang G. Tanshinone IIA affects the proliferation of A549/Tax by affecting the expression of MMP7 through the PI3K-AKT-mTOR signaling pathway. Discov Oncol 2025; 16: 369.

[33] Pandey P, Ramniwas S, Baldaniya L, Lakhanpal S, Mahmood D, Chaudhary K, Pandey S, Choi M, Choi J, Kim HJ, Ahn CH, Park MN, Khan F and Kim B. An updated review of molecular mechanisms implicated with the anticancer potential of diosgenin and its nanoformulations. Drug Des Devel Ther 2025; 19: 2205-2227.

[34] Grivennikov SI and Karin M. Dangerous liaisons: STAT3 and NF-kappaB collaboration and crosstalk in cancer. Cytokine Growth Factor Rev 2010; 21: 11-19.

[35] Detchou D and Barrie U. Interleukin 6 and cancer resistance in glioblastoma multiforme. Neurosurg Rev 2024; 47: 541.

[36] Lim HI, Kim GY, Choi YJ, Lee K and Ko SG. Uncovering the anti-cancer mechanism of cucurbitacin D against colorectal cancer through network pharmacology and molecular docking. Discov Oncol 2025; 16: 551.

[37] Méndez-Clemente A, Bravo-Cuellar A, González-Ochoa S, Santiago-Mercado M, Palafox-Mariscal L, Jave-Suárez L, Solorzano-Ibarra F, Villaseñor-García M, Ortiz-Lazareno P and Hernández-Flores G. Dual STAT-3 and IL-6R inhibition with stattic and tocilizumab decreases migration, invasion and proliferation of prostate cancer cells by targeting the IL-6/IL-6R/STAT-3 axis. Oncol Rep 2022; 48: 138.

[38] Berkley K, Zalejski J and Sharma A. Targeting STAT3 for cancer therapy: focusing on Y705, S727, or dual inhibition? Cancers (Basel) 2025; 17: 755.

[39] Wei R, Song J, Pan H, Liu X and Gao J. CPT1C-positive cancer-associated fibroblast facilitates immunosuppression through promoting IL-6-induced M2-like phenotype of macrophage. Oncoimmunology 2024; 13: 2352179.